PRISM Software: Processing and Review Interface for Strong-Motion Data

by Jeanne Jones, Erol Kalkan, Christopher Stephens, and Peter Ng

ABSTRACT

A continually increasing number of high-quality digital strong-motion records from stations of the National Strong Motion Project (NSMP) of the U.S. Geological Survey, as well as data from regional seismic networks within the United States, calls for automated processing of strong-motion records with human review limited to selected significant or flagged records. The NSMP has developed the Processing and Review Interface for Strong Motion data (PRISM) software to meet this need. In combination with the Advanced National Seismic System Quake Monitoring System (AQMS), PRISM automates the processing of strong-motion records. When used without AQMS, PRISM provides batch-processing capabilities. The PRISM software is platform independent (coded in Java), open source, and does not depend on any closed-source or proprietary software. The software consists of two major components: a record processing engine composed of modules for each processing step, and a review tool, which is a graphical user interface for manual review, edit, and processing. To facilitate use by non-NSMP earthquake engineers and scientists, PRISM (both its processing engine and review tool) is easy to install and run as a stand-alone system on common operating systems such as Linux, OS X, and Windows. PRISM was designed to be flexible and extensible to accommodate implementation of new processing techniques. All the computing features have been thoroughly tested.

INTRODUCTION

A continually increasing number of high-quality digital strong-motion records acquired from stations of the National Strong Motion Project (NSMP) of the U.S. Geological Survey (USGS), as well as data from regional seismic networks within the United States, calls for automated processing of strong-motion records with human review limited to selected significant events or to events identified as being problematic during automatic processing. The NSMP has developed the Processing and Review Interface for Strong Motion data (PRISM) software to meet this need, and to replace the outdated software program BAP (Basic Strong-Motion Accelerogram Processing; Converse and Brady, 1992) developed and used by the NSMP to process earthquake strong-motion records.

The PRISM software consists of two major components: a module-based record processing engine, and a review tool—a graphical user interface (GUI)—to manually review, edit, and process records. NSMP implements PRISM in a structured workflow environment that includes an instance of the Advanced National Seismic System Quake Monitoring System (AQMS) to automatically acquire and process strong-motion records. PRISM can also operate in a batch-processing mode. The PRISM software is platform independent (coded in Java), open source, and does not depend on any closed-source or proprietary software. To facilitate use by earthquake engineers and scientists, the PRISM processing engine and review tool are easy to install and run as a stand-alone system on common operating systems such as Linux, OS X, and Windows. PRISM was designed to be flexible and extensible to accommodate implementation of new processing techniques. The processing engine implements each processing step according to a well-defined application-programming interface (API) to allow incorporation of alternative implementations of each step.

Input to PRISM is currently limited to data files in Consortium of Organizations for Strong Motion Observation Systems (COSMOS) V0 format (COSMOS, 2001), so that all acceleration input time series need to be converted to this format. COSMOS V0 files contain raw acceleration time-series data in digital counts. All associated metadata, and particularly instrument response parameters, should be in the COSMOS V0 headers. In addition, earthquake magnitude is required for selecting appropriate band-pass filter corners. Output products include files in COSMOS V1 (raw acceleration time series in physical units with mean removed), V2 (baseline-corrected and filtered acceleration, velocity, and displacement time series), and V3 (response spectra, Fourier amplitude spectra [FAS], and common earthquake-engineering intensity measures [IMs]) formats.

PRISM joins a suite of tools also used by other ground-motion processing software (e.g., BAP, Converse and Brady, 1992, SeismoSignal, SeismoSoft, 2016), even though this software certainly has features not present in others. This article presents an overview of PRISM 1.0.0, including the processing engine and the review tool; updated PRISM versions will follow a sequenced-base major.minor.patch version identifier. All the computing features of PRISM have been thoroughly tested. Details of PRISM, including the configuration file format, how to run PRISM, output log files, and a performance assessment, can be found in Jones et al. (2017).

The complete list of abbreviations and symbols used throughout this article is given in Table 1.

	Table 1
	List of Abbreviations and Symbols Present in This Article
ABC	Adaptive baseline correction
AIC	Akaike information criterion
AQMS	Advanced National Seismic System Quake Monitoring System
API	Application programming interface
BAP	Basic strong-motion Accelerogram Processing software (see Data and Resources).
COSMOS	Consortium of Organizations for Strong-Motion Observation Systems (see Data and Resources)
f	Frequency
FAS	Fourier amplitude spectrum
FFT	Fast Fourier transform
f_{hc}	High-cut corner frequency
f_{lc}	Low-cut corner frequency
GUI	Graphical user interface
IM	Intensity measure
M	Moment magnitude
M_L	Local magnitude
n	Filter order
n_p	Polynomial order
N	Number of data points in the input time series
N_{taper}	Number of data points in full cosine taper
NSMP	National Strong Motion Project (see Data and Resources)
$P_{Phase}P_{icker}$	P-phase onset time picker
PRISM	Processing and Review Interface for Strong Motion data software (see Data and Resources)
rmsd	Root mean square deviation
$\overline{rmsd}$	Square root of the sum of the squares of root mean square deviation
SNR	Signal-to-noise ratio
samples/s	Samples per second
SRSS	Square root of the sum of the squares
QC	Quality check
T_{pad}	Total length of zeros in padding
t	Time instant
t_p	Event onset
t_1	Ending time of first polynomial in adaptive-baseline correction
t_2	Beginning time of second polynomial in adaptive-baseline correction
V0	COSMOS Volume 0
V1	COSMOS Volume 1
V2	COSMOS Volume 2
V3	COSMOS Volume 3
Y	Filter response
X_n	Difference between the velocity time series and the baseline fit
wt	Weight function
ω	Cyclic frequency
Δt	Sampling interval of time series in seconds
Δt_{ABC}	Sampling interval as number of samples in adaptive-baseline correction

PRISM PROCESSING ENGINE

The main features of the PRISM processing engine are as follows:

- platform-independent, modular, extensible, open-source software;
- fully automated;
- customizable processing parameters using a configuration file;
- resampling in the frequency domain;
- phase arrival time and maximum amplitude picking;
- processing in the time domain for mean removal, integration, and differentiation;
- acausal band-pass filtering;
- a baseline correction computed in the velocity domain, with its derivative applied as a baseline correction to the acceleration waveform;
- generation of products that include compatible acceleration, velocity and displacement time series, response spectra, FAS, and standard earthquake-engineering IMs. (Compatible data products include the initial values required to reliably reproduce all products using the released acceleration and without the need to pad the time series.);
- log files for quality control and reproducibility;
- for input, currently uses COSMOS V0 input format with metadata in COSMOS headers;
- products in COSMOS data format (V1, V2, and V3); and
- can be integrated into other strong-motion processing applications (e.g., a GUI for manually reviewing, editing, and processing).

The processing steps in the automated workflow are clearly defined. A set of conservative default parameters—specified in a configuration file—are used to generate V1, V2, and V3 data products. The processing includes quality assurance steps to flag particular records that may require further review by an analyst, and manual tuning of processing parameters in the GUI.

STRONG-MOTION RECORD PROCESSING

PRISM automatically processes acceleration records on a channel-by-channel basis using a well-defined set of steps based on generally accepted practices in strong-motion record processing (e.g., Shakal *et al.*, 2003, 2004; Stephens and Boore, 2004; Boore and Bommer, 2005; COSMOS, 2005). These steps, which are hardwired in the software, are described under V1, V2, and V3 processing.

Volume 1 (V1) Processing

Data in digital counts are converted to physical units, and the mean of the entire raw acceleration time series is removed. Figure 1 illustrates the corresponding workflow to generate the uncorrected acceleration history. A full instrument response correction is not applied because the sensor response is flat to direct current, and the cutoff frequency of the low-pass filter applied in V2 processing typically is lower than that of the natural frequency of an accelerometer (> 50 Hz). Instead, a
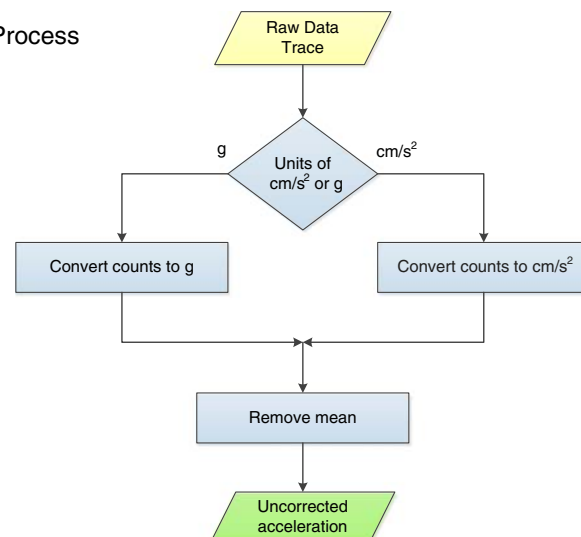
▲ **Figure 1.** Flowchart showing volume 1 (V1) data processing adopted for raw acceleration time series to produce uncorrected acceleration time series in physical units. The color version of this figure is available only in the electronic edition.

simple scaling factor is used (Graizer, 2015). Note that PRISM is not intended to process records with a lower natural frequency (< 50 Hz).
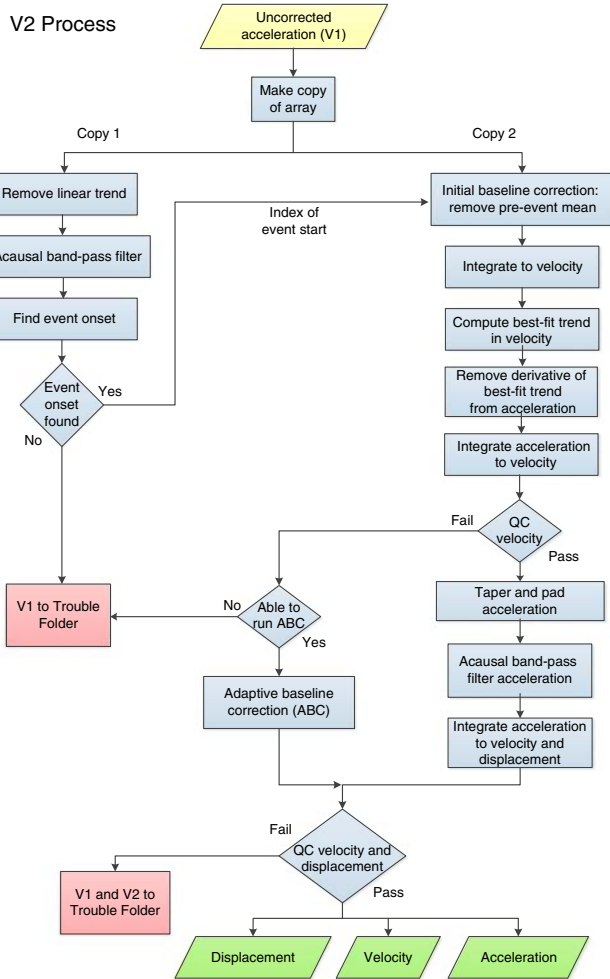
Volume 2 (V2) Processing

Corrected acceleration, velocity, and displacement time series are obtained by applying prescribed baseline correction methods and filtering to ensure that the spectral content of the resulting products is within the range of the sensors' frequency response and has a signal-to-noise ratio (SNR) well above that of expected background noise level.

The first step is to check the sampling rate of the acceleration time series. If the V1 acceleration has low time resolution less than about 200 samples/s, the time series is resampled to 200 samples/s in the frequency domain (as described in appendix A of Jones *et al.*, 2017) prior to V2 processing to reduce numerical noise (Kalkan and Stephens, 2017).

The V2 processing flow (Fig. 2) involves the following steps:

1. detect event onset;
2. remove pre-event mean from acceleration;
3. integrate to velocity;
4. compute best-fit trend in velocity record;
5. compute derivative of best-fit trend to velocity, remove from acceleration, and integrate baseline-corrected acceleration to velocity;
6. perform quality check (QC) of velocity record;
7. taper and pad acceleration record to condition for filtering;
8. apply acausal band-pass filter to acceleration in the time domain;
9. integrate filtered acceleration and check for ill-behaved velocity records; apply an adaptive baseline correction (ABC) as needed;

▲ **Figure 2.** Flowchart showing volume 2 (V2) data processing adopted for uncorrected acceleration time series to produce corrected acceleration, velocity, and displacement. The color version of this figure is available only in the electronic edition.

10. compute velocity and displacement from processed acceleration; and
11. perform QC on final velocity and displacement.
    These steps are explained in more detail in the following subsections.

Step 1: Event Onset Detection
The pre-event interval of the time series is useful for determining both a suitable initial-baseline correction and the spectral character of the background noise. Currently, PRISM has two options for computing t_p, the P-phase arrival time, which is the event onset time: the $P_{Phase}P_{icker}$ (Kalkan, 2016) and the Akaike information criterion (AIC) picker (Maeda, 1985). Details of these two pickers are discussed in appendix B of Jones *et al.* (2017).

Step 2: Pre-Event Mean Removal from Acceleration
Prior to integration to velocity, the mean of the pre-event interval, which extends from the beginning of the record to a prescribed offset prior to t_p (to allow for uncertainty in computing

t_p; the default for this parameter is 0 s, but is configurable), is subtracted from the entire uncorrected acceleration time series.

Step 3: Integrate to Velocity
The trapezoidal rule is used to integrate from acceleration to velocity. In each integration step, the unknown initial value introduces a linear trend in the result that, on a physical basis, is expected to have a slope near zero. The slope of the trend is equal to the unknown initial value. Thus, after the initial integration, the slope of the pre-event interval is then used as an estimate of the initial value, and a correction is made to the integrated time series.

Step 4: Compute Best-Fit Trend in Velocity
Low-frequency noise of both natural and instrumental origin is present in nearly all strong- and weak-motion records (Trifunac, 1971; Graizer, 1979; Boore *et al.*, 2002). This noise becomes readily apparent in the form of long-period wandering or monotonic drift from zero in velocity and displacement time series obtained by single and double integration, respectively, of acceleration. The process of integration itself introduces additional low-frequency noise. The variety and complexity of the noise sources preclude designing an all-encompassing correction scheme (Graizer, 2010).

Physically, the mean of the velocity time series should be near zero at the start and end of the record. To choose an appropriate baseline correction to achieve a zero mean of the velocity record, PRISM first calculates the root mean square deviation (rmsd) for two functions: a simple linear regression and a second-order polynomial regression. rmsd is a statistical measure of the scatter of data about the mean of a collection of data samples, and it is computed as

$$\text{rmsd} = \sqrt{\frac{1}{N}\sum_{n=1}^{N}[X_n(t)]^2}, \tag{1}$$

in which X_n is the difference between the velocity and the fit, t is time instant, and N is number of data points. The function with the smallest rmsd is selected as the baseline correction.

Step 5: Remove Derivative of Best-Fit Trend in Velocity from Acceleration
The derivative of the best-fit trend computed in the velocity domain is applied as the baseline correction to acceleration time series by subtracting it. After making this correction, the acceleration record is integrated to velocity and reviewed for quality.

Step 6: QC for Velocity
On the basis of physical plausibility, the velocity prior to the earthquake onset and after the interval of strong motion is expected to oscillate around zero. To satisfy these criteria, the following quality control steps are applied to the velocity record.
1. *Step 6a*: Determine a suitable window length for intervals at the beginning and the end of the velocity time series for the QC as

window length $=$ max(length of pre

$$- \text{event interval}, 1/f_{\text{lc}}), \qquad (2)$$

in which f_{lc} is low-cut corner frequency (explained below). For the leading velocity interval, find the mean from the start of the time series to the end of the initial window; for the final trailing velocity interval, find the mean from the first zero crossing after the start of the interval to the end of the time series.

2. *Step 6b*: Compare these two means against QC thresholds specified in the configuration file. QC passes if both leading and trailing means are less than or equal to the thresholds. Default threshold values, which can be changed in the configuration file, are as follows:

Leading velocity threshold $= 0.01$ cm/s

Trailing velocity threshold $= 0.01$ cm/s.

Step 7: Tapering and Padding
Filtering is performed in the time domain. Time-domain filtering assumes that the time series is zero-valued outside of the data interval. To accommodate filter transients from bidirectional acausal filtering, the data time series are temporarily extended with zero padding at both the leading and trailing edges. Following Converse and Brady (1992), the total length of the zero padding (T_{pad}) in seconds is determined using the following formula:

$$T_{\text{pad}} = 1.5n/f_{\text{lc}},$$

in which n is the order of the Butterworth filter. In a typical case in which $n = 4$ and $f_{\text{lc}} = 0.1$ Hz, T_{pad} should be 60 s. Thus, the time series is extended symmetrically at both ends with zero padding, each of duration $T_{\text{pad}}/2$, or 30 s in this example. In Figure 3, T_{pad} is presented as a function of n for the three values of f_{lc} (0.1, 0.3, and 0.5 Hz) currently used for time-domain filtering (see Table 2).

To avoid the introduction of spurious low-frequency noise from any discontinuity between the signal and the padding (i.e., a jump in the value or a change in the gradient), cosine tapers are applied to the ends of the data intervals so that there are smooth transitions to zero in which they abut the zero pads. The width of the full cosine taper, N_{taper} (in samples), is taken as the number of samples from the beginning of the record to the last zero crossing before the event onset. The weights wt, as a function of sample index i, are computed by

$$wt(i) = \frac{1}{2}\left[1 - \cos\left(\pi \frac{i}{N_{\text{taper}}/2}\right)\right], \qquad i = 0, N_{\text{taper}}/2 - 1$$

$$(4a)$$
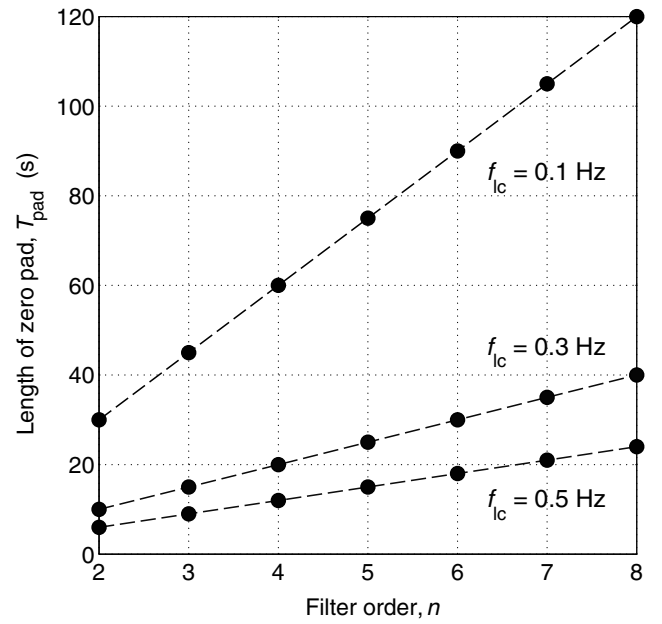
▲ **Figure 3.** Graphs showing total length of zeros (T_{pad}) added to the record as a function of acausal (two-pass) Butterworth filter order (n) and low-cut corner frequency (f_{lc}). In time-domain filtering, half of T_{pad} is added to the front and half to the back of the time series. Note that the original record after padding is longer in duration by T_{pad}. These pads are necessary whether the filtering is performed in the time or frequency domain. This figure is modified from figure 3 in Boore (2005).

$$wt(i) = \frac{1}{2}\left[1 + \cos\left(\pi \frac{i - \left(N - \frac{N_{\text{taper}}}{2}\right) + 1}{N_{\text{taper}}/2}\right)\right],$$

$$i = N - N_{\text{taper}}/2, N - 1, \qquad (4b)$$

in which N is the total number of data samples in the time series.

Note that to maintain compatibility, the padded sections of the filtered acceleration are retained when deriving velocity, displacement, and response spectra. For computing the FAS, the zero pads are extended so that the total number of data points is a power of 2. All time-series pads are removed after final processing for dissemination of the V2 products. The reasons for this practice are to reduce file size (the padded segments of the data—filter transients—can be long and have small amplitudes in the acceleration time series), and to avoid the misinterpretation that the transient motions before and after the recorded data represent actual motion. Note that acausal filtering also introduces apparent pre-event motions in the retained time series. Removing the pads after filtering can result in incompatibilities and biases in quantities derived from pad-stripped accelerations (Boore *et al.*, 2012). One way of overcoming this incompatibility is to provide the initial values of the processed time series in the V2 and V3 file headers so that if a user needs to obtain velocity by directly integrating the acceleration time series in the V2 file, the initial value stored in

Table 2			
Magnitude Dependent Band-Pass Filter Corner Frequencies			
Earthquake Local Magnitude (M_L)	**Low-Cut Corner Frequency, f_{lc} (Hz)**	**High-Cut Corner Frequency, f_{hc} (Hz)**	**Nyquist Frequency (Hz)**
$M_L \geq 5.5$	0.1	40	50
$3.5 \leq M_L < 5.5$	0.3	35	45
$M_L < 3.5$	0.5	25	30

the header should be added to the integration as a constant. Similarly, in computing the displacement, the initial value for displacement also needs to be considered. The PRISM processing engine also offers an option in the configuration file to write out time series with filter transients.

Step 8: Band-Pass Filtering
It was found during the development stage that when band-pass filters are applied in velocity rather than in acceleration, the resultant amplitudes of higher frequencies are systematically low. This is because integration acts as a low-pass filter (Kalkan and Stephens, 2017). PRISM now applies band-pass filters in acceleration to avoid this distortion in the frequency content of the signals. Acausal filtering is achieved by running a causal Butterworth filter forward and then backward in the time domain. In strong-motion processing, acausal filtering is generally preferred over causal filtering to avoid phase distortion in the signal (Boore and Akkar, 2003; Bazzurro et al., 2005); causal filtering is not an option in PRISM. The acausal filter is applied in the time domain by convolution of its transform with the time history. Following Kanasewich (1981), the response of a low-cut acausal Butterworth filter is defined as

$$Y = \frac{(f/f_{lc})^{2n}}{1 + (f/f_{lc})^{2n}} \tag{5}$$

and high-cut acausal Butterworth filter is

$$Y = 1 - \frac{(f/f_{hc})^{2n}}{1 + (f/f_{hc})^{2n}}, \tag{6}$$

in which Y is filter response (0–1), f is frequency, n is filter order. Selecting n is a compromise between effectively removing unwanted low-frequency noise and avoiding the excessive ringing caused by using too high of an order. In PRISM, the default value for n is 4, which can be overwritten in the configuration file.

In strong-motion data processing, and at least for ground-motion reference sites, it is desirable to use the broadest frequency bandwidth with a high SNR. When the SNR is sufficiently high—at least twice as high as the background—a simple low-cut filter can usually eliminate the part of the signal contaminated by long-period noise (Trifunac, 1971). The tran-

sition bands of a Butterworth filter at typical low- and high-frequency corners and for a range of filter orders are shown in Figure 4. Methods for selecting an appropriate low-cut filter corner are generally subjective, but often are based on approaches such as a comparison between the FAS of the record with that of a model of the noise or the amplitude spectrum of the pre-event time window (Trifunac, 1977; Shakal and Ragsdale, 1984); a comparison between the behavior of the Fourier spectrum of the earthquake signal at long periods to that expected from theoretical models—at long periods the FAS is expected to decay in proportion to f^{-2} (Brune, 1970, 1971); or the physical plausibility of the velocity and displacement time series obtained by integration, which requires a subjective manual review. For example, standard Pacific Earthquake Engineering Research Center manual processing practice makes use of all three approaches (Darragh et al., 2004; Ancheta et al., 2013). Another common approach is the use of the response spectrum for selecting the low-cut corner frequency (Shakal et al., 2004).

A high-cut filter is applied to remove high-frequency noise in the record, which commonly occurs in urban areas with high levels of background noise, or may be present due to contamination from 60 Hz alternating current power. The upper-frequency limit on the usable range of high frequencies in the record is typically controlled by setting the corner at 80% of the Nyquist frequency, which is at half of the sampling frequency.

When PRISM is run in automatic or batch mode, the high- and low-cut filter corner frequencies are preselected on the basis of the local magnitude (M_L) of the earthquake. The filter cutoff frequencies, presented in Table 2, are adapted and modified from Massa et al. (2010). It should be noted that the value of f_{hc} for $M_L \geq 5.5$ is valid for records with a sampling rate of at least 100 samples/s. The limits on sampling rates are presented in Table 2. If relative noise levels are high, it is important that f_{lc} values are chosen individually considering the noise level—based on where the amplitude of Fourier spectrum of the signal approaches to that of noise floor. This only can be done by resetting values in the configuration file or using the PRISM review tool.

Step 9: Adaptive Baseline Correction (ABC)
Strong-motion recordings may have physically implausible trends due to instrumental noise, such as spikes or step-like offsets in the baseline. The signals may also be contaminated by rotational or gravitational effects or by static displacements (e.g., Graizer, 2005; Boroschek and Legrand, 2006; Kalkan and Graizer, 2007a,b), particularly when instruments are located close to the fault rupture. Until recently, and even today, most strong-motion instruments record only three orthogonal translational motions, and there is no direct measurement of rotations, so that correcting for these effects is problematic. Over the years, a variety of techniques have been developed to address these issues, such as multisegment fitting with linear or low-order polynomials to velocity, to effectively remove them from the data (Graizer, 1979; Iwan et al., 1985; Boore, 2001; Boore et al., 2002; Kalkan and Kunnath, 2006). Graizer (1979)
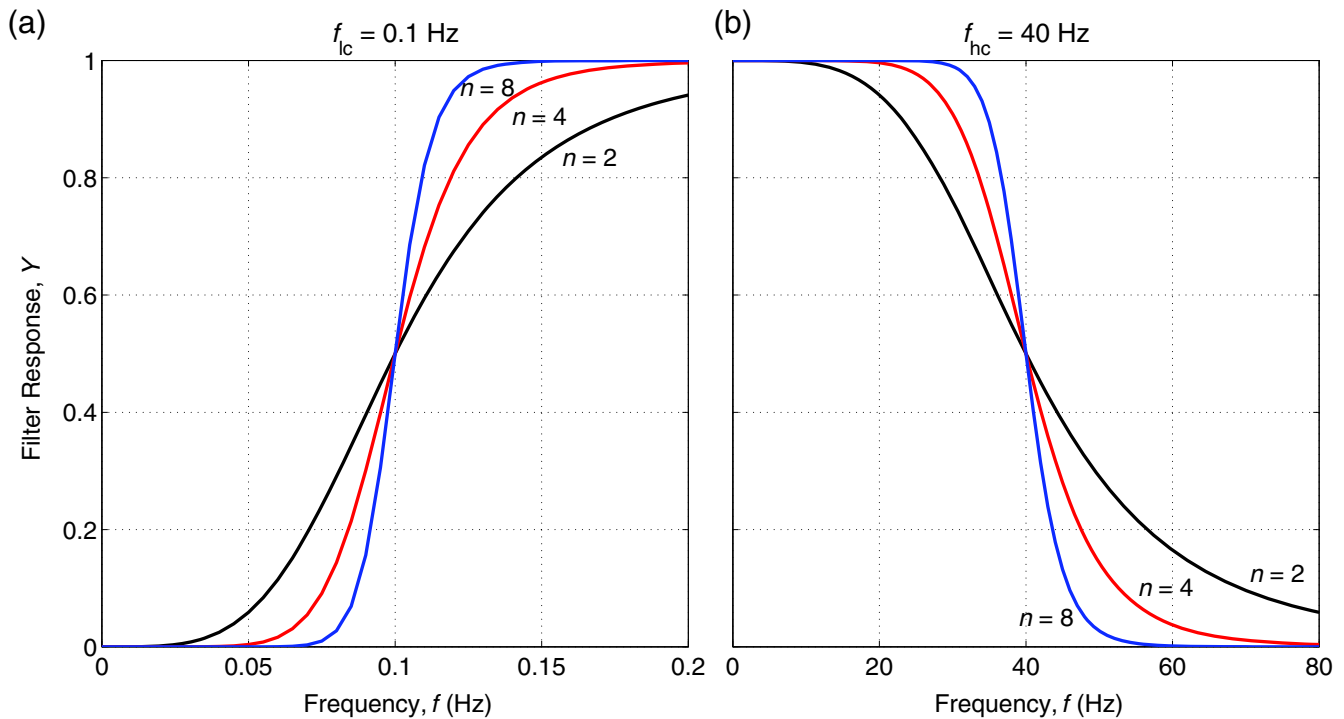
▲ **Figure 4.** Graphs showing as a function of frequency (a) a low-cut Butterworth filter with a low-cut corner f_{lc} of 0.1 Hz, and (b) a high-cut Butterworth filter with a high-cut corner f_{hc} of 40 Hz. The higher the filter order n, the more abrupt the cutoff. The color version of this figure is available only in the electronic edition.

proposed selecting among a series of progressively higher order polynomials to best fit the velocity time series. Iwan *et al.* (1985) proposed an alternative baseline-fitting scheme, in which the data window is divided into three segments with boundaries at times t_1 and t_2, which allows the leading and trailing velocities to be more readily constrained to oscillate around zero (a physical constraint). A problem with this method is making appropriate selections for t_1 and t_2. A common simplification is to assume that t_1 is equal to t_2 (i.e., there is only one baseline offset), and that the time of the offset corresponds to the intercept on the time axis of a line fit to the later part of the velocity time series. Although this seems to be a judicious solution for many records (Boore and Bommer, 2005), it may not be sufficient for records that in fact have multiple baseline irregularities, each requiring a different functional form to properly model.

PRISM incorporates an ABC scheme to address cases in which the initial baseline correction described in step 4 is not satisfactory. The ABC scheme, illustrated in Figure 5, is modified from the method of Iwan *et al.* (1985). In this scheme, a series of piecewise linear or higher order polynomials are fit to the velocity time series obtained in step 3 to remove or to diminish the long-period noise or drift in the signal. Specifically, the first step is to independently fit polynomials to the leading (0 to t_1) and trailing (t_2 to end) sections of the velocity time series, outside of the interval of strongest motions, during which rotational effects or the presence of static offsets are expected most likely to occur. These two polynomials, computed with a least-squares method, are connected by a cubic spline (between t_1 and t_2) (Wang, 1996).

In ABC, the time t_1 is set equal to t_p (the event onset time). Then, the ABC fitting routine uses a heuristic-based iterative method to determine optimal values for the time t_2 and the order of polynomials (n_p), such that the following requirements are satisfied:

1. a goodness-of-fit parameter should be minimized; and
2. boundary conditions should be met within specified tolerances. The boundary conditions are that the leading and trailing velocities and the trailing displacements should all oscillate around zero reference.

This method generates a sequence of approximate solutions by incrementing t_2 by the configurable parameter Δt_{ABC}, and by varying n_p over a range specified in the configuration file (currently 1 [linear] or 2 [quadratic] for the first polynomial, and 1 [linear] through 3 [cubic] for the second polynomial). Smaller Δt_{ABC} values yield more accurate results at the expense of increasing the processing time. The value of t_2 is constrained to be no closer to t_p than $1/f_{lc}$ to prevent the spline-fitting function from introducing an artifact. By trial-and-error test, it was determined that a value of Δt_{ABC} corresponding to 200 samples (independent of sampling rate) produces reasonably robust fits while maintaining acceptable processing times. The method is called convergent if the corresponding sequence minimizes the square root of the sum of the squares (SRSS) of rmsd, and the boundary conditions described above are met within the specified tolerances described in step 11 and given in the configuration file. For the entire velocity record, the rmsd considering three segments—first
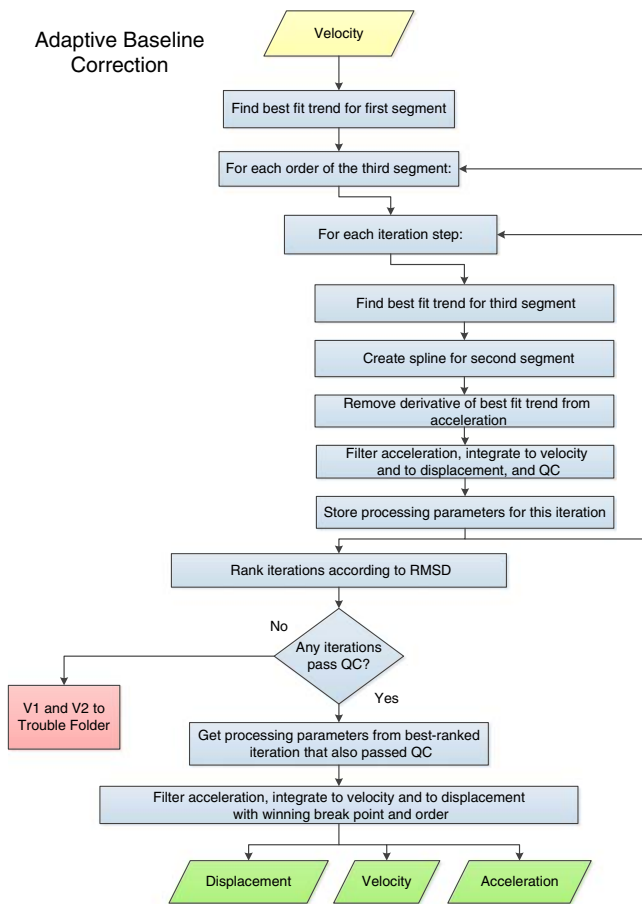
▲ Figure 5. Flowchart showing adaptive baseline correction (ABC) scheme in Processing and Review Interface for Strong Motion data (PRISM) for correcting velocity time series for which initial baseline correction is not satisfactory for removing implausible trends. The color version of this figure is available only in the electronic edition.

polynomial, spline, and second polynomial—is computed by taking SRSS of rmsd values of the three individual segments as

$$\overline{\mathrm{rmsd}} = \sqrt{\sum_{n=1}^{3} (\mathrm{rmsd}_n)^2}. \qquad (7)$$

After the ABC, any residual low-frequency noise is removed by band-pass filtering, as described in step 8.

To demonstrate how ABC works, Figure 6a displays a sample record—the north–south component of the acceleration recorded at the USGS Northern California seismic station JBR from the 2014 **M** 6.0 South Napa earthquake—after removal of the pre-event mean (step 2). Figure 6b shows the velocity obtained by integrating the adjusted acceleration (step 3), in which there is a clearly identifiable positive trend away from zero starting between about 90–100 s. The initial baseline correction (step 4) is applied to correct for the type of baseline shift shown in Figure 6b, and the resulting velocity is plotted in Figure 6c. Although the initial baseline correction removed the

apparent trend in a later part of the record (from ∼100 to 180 s), it distorted the beginning portion (0–33 s). This record failed in QC in step 6 because the average leading velocity is larger than the tolerance value (0.01 cm/s), and the record was flagged automatically for further processing by ABC.

The results for applying the ABC procedure are shown in Figure 7a. Starting with the velocity from step 3, the algorithm determined that a value of 43.3 s for t_2 and a second-order polynomial fits both the leading and trailing segments, thus providing an optimal fit to the data. The velocity time series is then recomputed by integrating the acceleration time series after removing the derivative of the best-fitting trend in velocity. In the end, the ABC procedure was able to remove the long-period distortions of the baseline visible in the uppermost plot shown in Figure 7a.

Step 10: Computation of Velocity and Displacement
Velocity and displacement are obtained by using the trapezoid rule for numerical integration of the corrected acceleration time series.

Step 11: QC for Final Velocity and Displacement
Using the same procedure described in step 6, PRISM finds the means of the leading and trailing velocity windows as well as the trailing displacement window, and compares these values against prescribed threshold values. QC passes if all three means are less than or equal to the thresholds values. Default threshold values for velocity are given in step 6, and it is 0.01 cm for trailing displacement.

It should be noted that strong ground motions recorded close to a fault rupture (generally within about 20 km) may contain static offsets (residual displacements) in displacement as a result of the faulting mechanism. Because of filtering, the automated processing does not retain such offsets; alternative methods not yet implemented in PRISM would need to be used to recover such offsets.

Volume 3 (V3) Processing
V3 processing involves computation of elastic response spectra, FAS, and earthquake-engineering IMs. The V3 processing, illustrated in Figure 8, is performed in either the time or frequency domain as appropriate.

Elastic response spectra (relative displacement, SD, relative velocity, SV, and absolute acceleration, SA) are computed following the numerical method of Nigam and Jennings (1969). The spectra are computed for 0%, 2%, 5%, 10%, and 20% of critical damping over a wide range of periods (0.04–15 s). The lower and upper bounds on spectral periods are independent of the band-pass filter corners. Pseudoacceleration and pseudovelocity spectra can be computed as $\omega^2 \times \mathrm{SD}$ and $\omega \times \mathrm{SD}$, respectively.

The FAS is computed by applying a fast Fourier transform (FFT) to the baseline-corrected and filtered acceleration time series from step 8 (or step 9, if implemented). The time series may be symmetrically extended with additional zero padding at the ends to ensure that the number of samples is a power of 2,
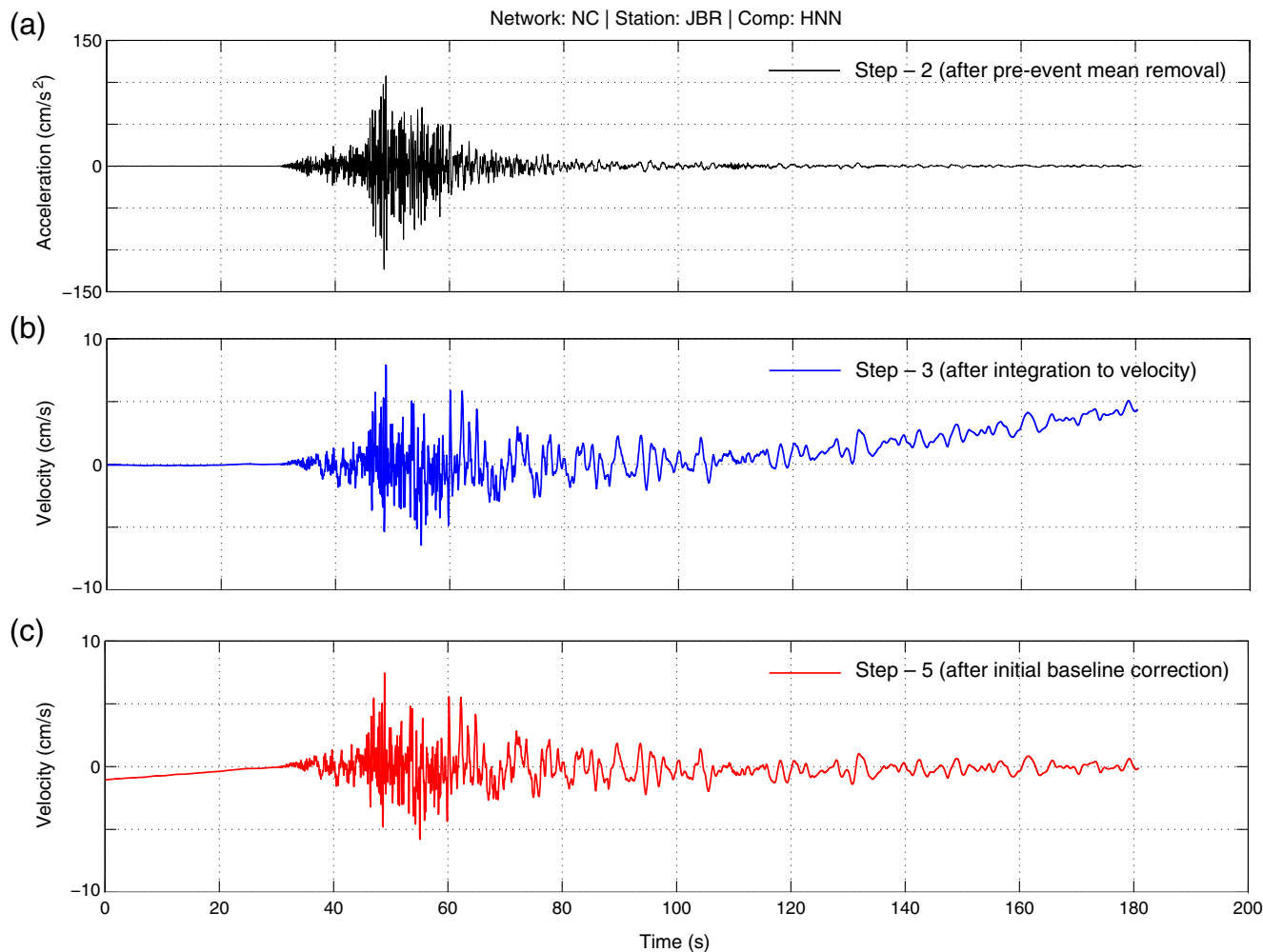
▲ **Figure 6.** Graphs showing (a) north–south component acceleration recorded at JBR from the 2014 **M** 6.0 South Napa earthquake, after removal of the pre-event mean from the whole record (step 2), (b) velocity from integration of the acceleration (step 3), and (c) velocity after initial baseline correction (step 5). Although the initial baseline correction removed the apparent trend in later part of the signal (∼100–180 s), it distorted the beginning portion (0–33 s). This record was flagged for further processing using the ABC scheme. The color version of this figure is available only in the electronic edition.

as is required by the FFT algorithm. A weighting function is applied to minimize spectral leakage (see equations 4a and 4b). Considering that FAS are computed for selected frequencies in the 0.066–25 Hz range (periods of 0.04–15 s), low sampling at high frequencies results in smoother FAS. In addition, a three-point smoothing is applied.

PRISM computes various earthquake-engineering IMs that are written to the headers of the COSMOS V3 files. These IMs are Arias intensity, bracketed duration, duration interval, response spectrum intensity, root mean square acceleration, and cumulative absolute velocity. Details on how these parameters are computed are given in Jones *et al.* (2017).

EXAMPLES OF V2 AND V3 PRODUCTS

The end products of PRISM are illustrated for two representative records from the 2014 **M** 6.0 South Napa earthquake, one with low amplitudes and one with high amplitudes. For the low amplitude record the final suite of acceleration, velocity, and displacement time histories (V2 products) is shown in Figure 9, and the pseudospectral acceleration, pseudospectral velocity, and displacement response spectra (V3 products) are presented in Figure 10. This record did not require ABC processing. The high-amplitude record, which did require ABC processing and subsequently passed QC, is displayed in Figure 11.

COMPARISONS AMONG PRISM, BAP, AND CSMIP PROCESSING

Systematic comparisons in both time and frequency domains were made between records automatically processed using PRISM and using BAP, and between PRISM products and records processed by California Strong Motion Instrumentation Program (CSMIP; Shakal *et al.*, 2003, 2004). The set of test records includes representative input motions with varying
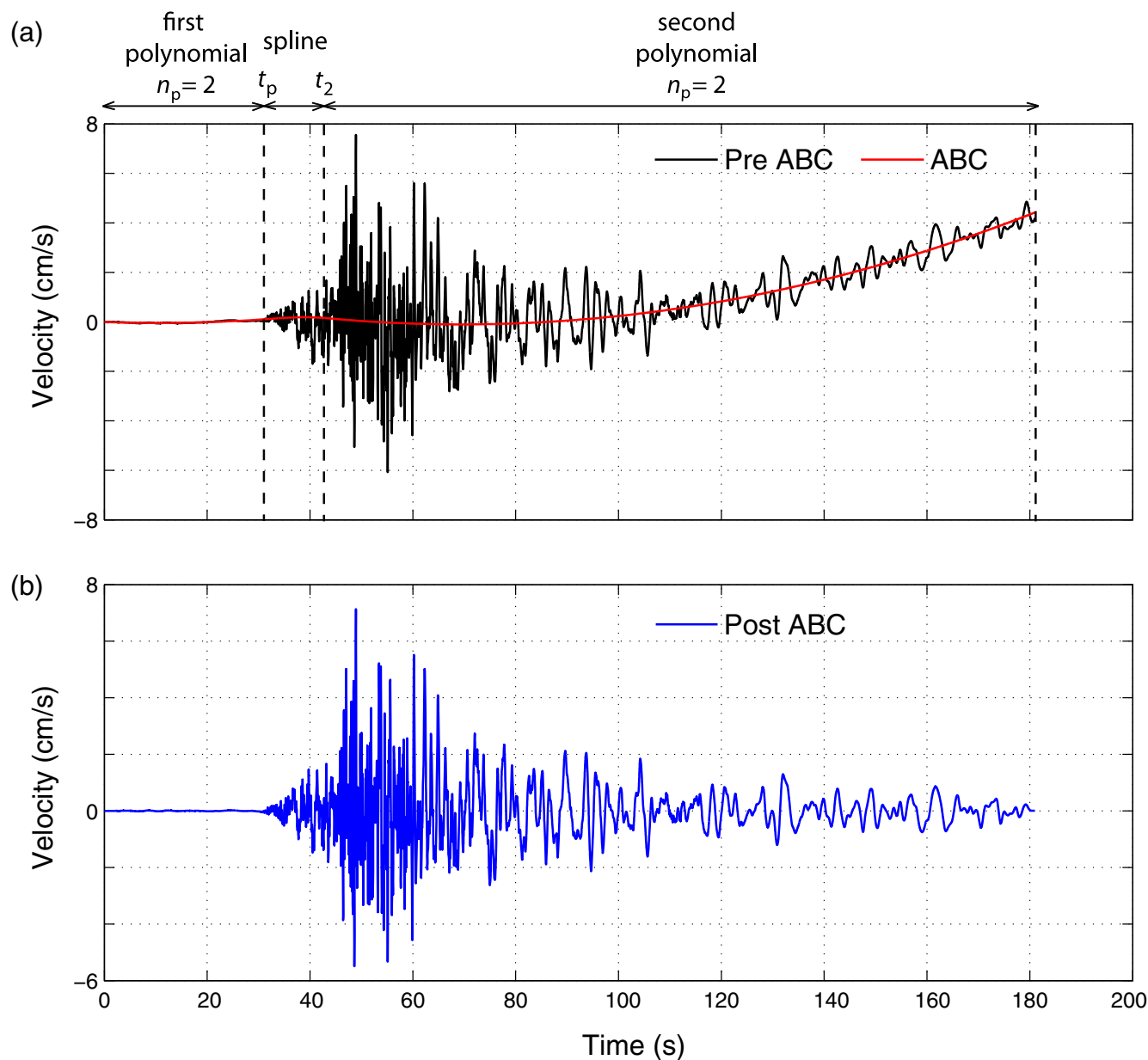
▲ **Figure 7.** Graphs showing (a) uncorrected velocity and adaptive-baseline fit. The baseline fit consists of a quadratic ($n_p = 2$) polynomial fit to the velocity from 0 to event onset (t_p) at 33.3 s, a quadratic polynomial fit from $t_2 = 43.3$ s to the end of the record, and a cubic spline connecting these two polynomials between t_p and t_2. (b) Velocity with the computed ABC, which does not show visible long-period distortions. The sampling rate is 200 samples/s. The color version of this figure is available only in the electronic edition.

resolutions, frequency content, and amplitudes. Attempts were made to match the processing parameters as closely as possible, but some small differences between the processed records are expected because of fundamental differences in the techniques used. For example, PRISM uses Butterworth acausal filtering at both low and high frequencies and processes in the time domain, whereas in BAP a low-frequency acausal Butterworth filter is applied in the time domain, but at high-frequencies BAP applies a cosine taper in frequency domain. In CSMIP processing, an initial long-period filter is applied to the instrument-corrected acceleration data, and then velocity and displacement are sub-

sequently acquired by integrating the acceleration, and are filtered using the same long-period filter (Shakal *et al.*, 2004). In contrast, PRISM applies filtering to corrected acceleration only, and velocity and displacement are obtained by integrating the filtered acceleration to provide compatible products. Despite differences in the details of the processing procedures, it is shown in Kalkan and Stephens (2017) that, for each component and within the frequency passband common to these procedures, there are only minor differences among the waveforms.

A comprehensive statistical evaluation considering more than 1800 ground-motion components demonstrates that
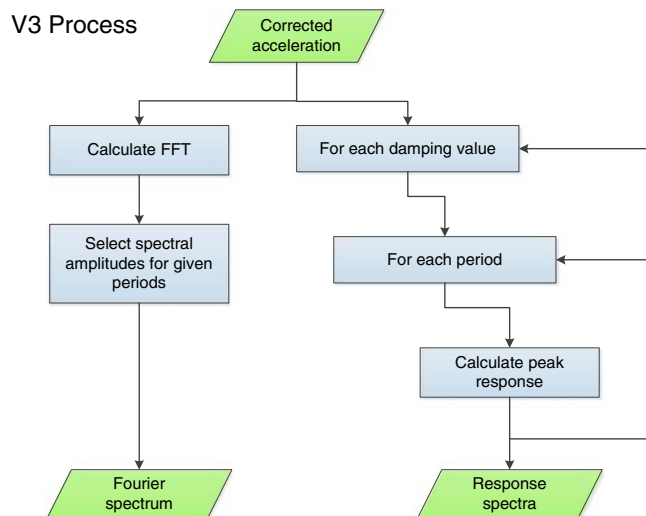
V3 Process

▲ **Figure 8.** Flowchart showing volume 3 (V3) data processing using corrected acceleration time series to produce elastic response spectra for pseudoacceleration, velocity, and displacement at different damping values, and Fourier amplitude spectrum. The color version of this figure is available only in the electronic edition.

differences in peak amplitudes of acceleration, velocity, and displacement time series obtained from PRISM and CSMIP processing are less than 4% for 99% of the data, and are equal to or less than 2% for 96% of all data. Other statistical measures, including Euclidean distance (L2 norm) and windowed root mean square levels of processed time series, also indicate that both schemes generate comparable products. The results of this evaluation study are presented in Kalkan and Stephens (2017).

PRISM REVIEW TOOL

The PRISM review tool is a desktop application that provides an interactive GUI for visually inspecting, editing, and processing COSMOS V1 data to create corresponding new or revised V2 and V3 data products. The tool utilizes the PRISM processing engine API to handle manual editing and processing tasks as well as calling upon the API to generate COSMOS data products. Developed using open-source technologies and the Java programming language, the review tool can be deployed on multiple operating system platforms, including Windows (v. 7 or later), Linux, and Mac OS X.

The main interface of the tool (Fig. 12) provides standard menu and toolbar options for performing common tasks, including setting application preferences, loading COSMOS files, running plots, navigating generated plot sets, and editing. The interface comprises several panels, including the *Node Explorer*, *Content Area*, *Properties*, and *Status*. The *Node Explorer* displays a hierarchical tree structure of nodes denoting COSMOS files currently loaded into the application. The structure stratifies the nodes by event name, station code, COSMOS file data type, and file names. The *Content Area* is the area in

which generated plots are displayed. The viewer comprises two tab pages that display seismic trace plots and spectral trace plots, respectively. The *Properties* panel displays a table of various attributes that pertain to a file that is currently selected in the *Node Explorer*. Finally, the *Status* panel displays output messages that are generated during runtime.

Editing can be performed in either the time domain (for applying baseline corrections) or the spectral domain (for selecting band-pass filter corners) of a selected file. Separate editors named the *Seismic Editor* and *FAS Editor* (Fig. 13) are used to perform editing and processing of seismic and spectral data, respectively. Editing of seismic data is initiated by either right clicking a selected file in *Node Explorer*, then selecting *Edit* from the context menu that appears, or by selecting the seismic plot corresponding to the selected file, then right clicking and selecting *Edit* from the plot's own context menu. Similarly, editing of spectral data is initiated by selecting a spectral plot corresponding to a specific group of files of acceleration data, then right clicking and selecting *Edit* from its context menu.

The *Seismic Editor* takes either a V1 or V2 file as input, then uses the V1 file (retrieving it as necessary when the source input was a V2 file) and creates a temporary V2 process object that contains acceleration, velocity, and displacement data. These data are used to create the initial plots that are displayed at startup. Editing of seismic data consists of baseline correction and band-pass filtering. Note that as each operation is performed, the operation is recorded into the table located to the right of the editor. Clicking on a step item in the table will take processing back to that particular step, and subsequent operations that follow will then override steps previously taken after that step. After baseline correction comes filtering (Fig. 13b), which involves setting the low and high filter range values. This step is performed by clicking *Edit*, which opens the *Filter Editor* dialog showing the spectral view of the acceleration data and the currently set low and high filter range values that can be edited. The last step in the editing process is to commit the changes by clicking *Commit*, which then generates and stores new or revised V2 and V3 data products. All of the accepted processing steps are stored as comments in the V2 and V3 products so that the results can be reproduced.

CONCLUDING REMARKS

A robust automated data processing procedure is essential to ensure high-quality accelerograms and derived products for immediate use in earthquake-engineering applications and for seismological studies. In this article, the automated PRISM software developed at the USGS is described. Although there are no unique procedures for strong-motion data processing, PRISM utilizes widely accepted techniques (e.g., Shakal *et al.*, 2003, 2004; Stephens and Boore, 2004; Boore and Bommer, 2005; COSMOS, 2005) that are designed to remove low- and high-frequency noise to provide reliable estimates of velocity and displacement time series. All of the essential steps applied in PRISM, whether automatic or manual, are documented in

Network: NC | Station: C002 | Comp: HNE
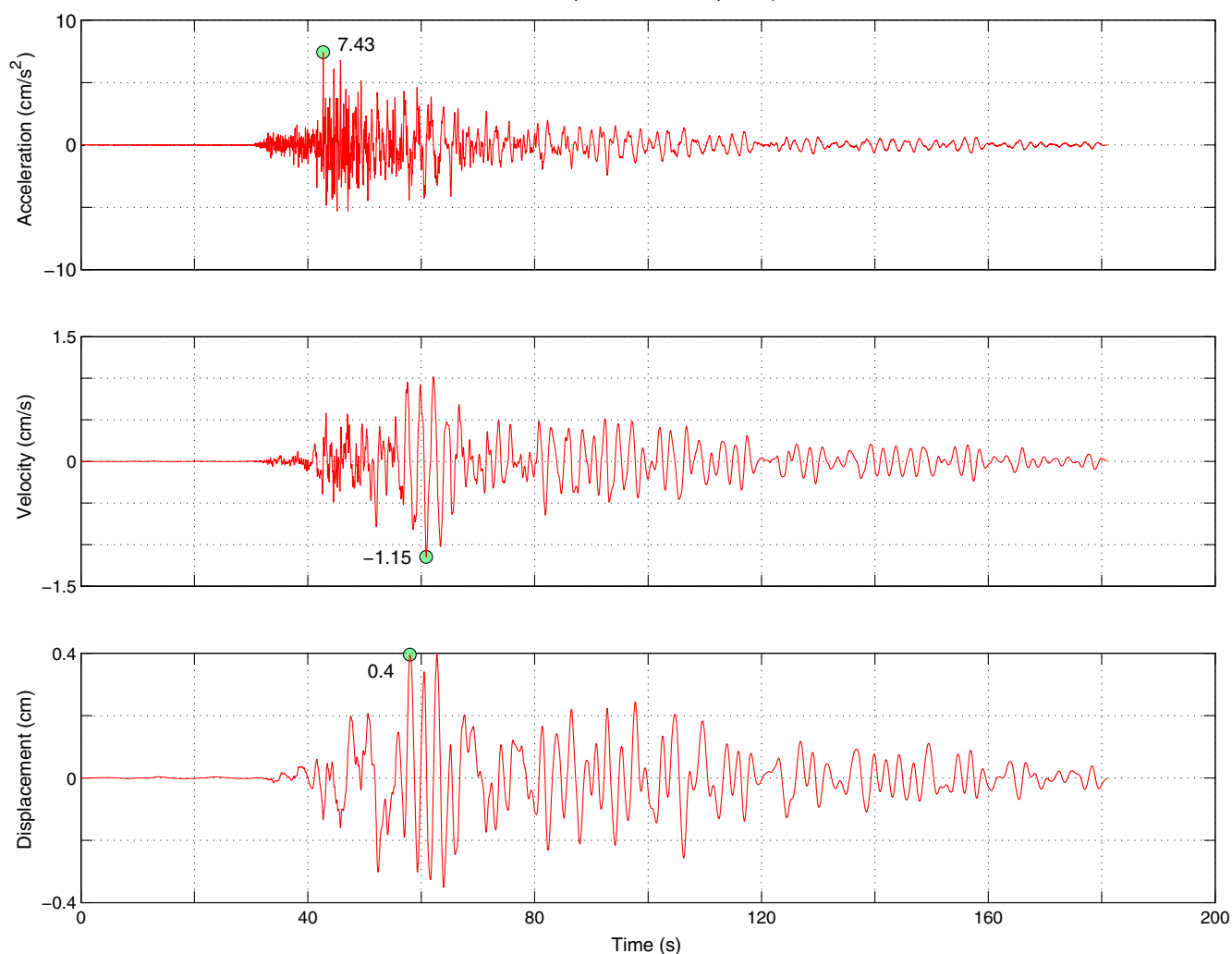
▲ **Figure 9.** Graphs showing a final suite of acceleration, velocity, and displacement time series (V2 products) for channel HNE at station C002 recorded with 200 samples/s from the 2014 **M** 6.0 South Napa earthquake in California. Note that this channel of the record was processed without a need for adaptive-baseline correction. Circles indicate the peak values of V2 products. The color version of this figure is available only in the electronic edition.

the ASCII file headers of the processed time series so that users can evaluate the suitability of the data for their intended application.

Complementary to the California Integrated Seismic Network (see Data and Resources), in which automated processing of records provides metadata that are used as input for products such as ShakeMaps, the PRISM processing engine was designed to automatically and rapidly generate preliminary products of earthquake-engineering interest to include in the Internet Quick Reports issued by the Center for Engineering Strong Motion Data (see Data and Resources).

DATA AND RESOURCES

Processing and Review Interface for Strong Motion data (PRISM) software for both the processing engine and the review tool is available at http://earthquake.usgs.gov/research/ software/#prism (last accessed February 2017). Users are encouraged to e-mail the authors with evidence of any problems or errors encountered while running PRISM. The unprocessed ground-motion data from the 2014 **M** 6.0 South Napa Earthquake used in demonstration of PRISM are available at the Center for Engineering Strong Motion Data (http://www.strongmotioncenter.org; last accessed February 2017). The California Integrated Seismic Network website is available at http://www.cisn.org/ (last accessed February 2017). The Basic strong-motion Accelerogram Processing (BAP) software is available at https://escweb.wr.usgs.gov/nsmp-data/processing.html#BAP (last accessed February 2017). The Consortium of Organizations for Strong-Motion Observation Systems (COSMOS) website is available at http://www.cosmos-eq.org/ (last accessed February 2017). The National Strong Motion Project (NSMP) website is available at http://earthquake.usgs.gov/monitoring/nsmp/ (last accessed February 2017). ⬚
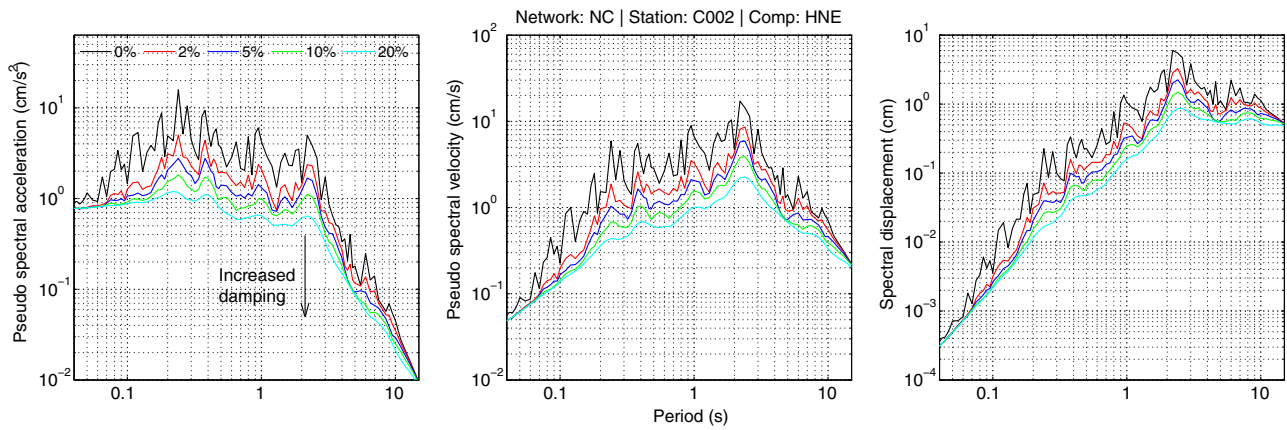
▲ **Figure 10.** Graphs showing a final suite of pseudospectral acceleration, pseudospectral velocity, and spectral displacement spectra computed at different damping levels (0%, 2%, 5%, 10%, and 20% of critical) for three channels of C002 record with 200 samples/s from the 2014 **M** 6.0 South Napa earthquake in California. The color version of this figure is available only in the electronic edition.
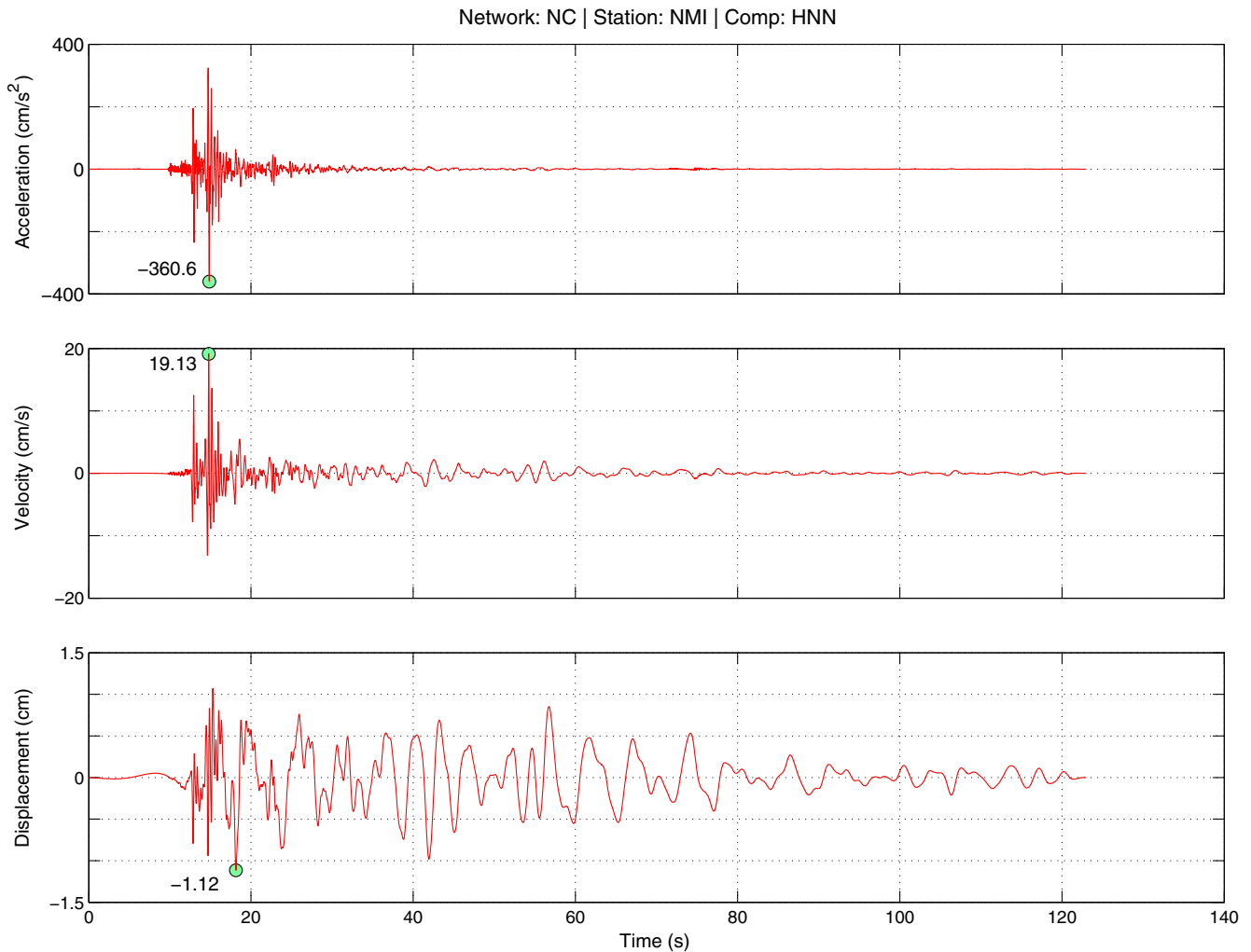
▲ **Figure 11.** Graphs showing a final suite of acceleration, velocity, and displacement time series (V2 products) for channel HNN at station NMI recorded with 100 samples/s from the 2014 **M** 6.0 South Napa earthquake in California. Note that this channel of the record was processed with adaptive-baseline correction. Circles indicate the peak values of V2 products. The transient on the displacement before the earthquake onset is an inherent feature of acausal filtering, as is particularly evident for impulsive signals. The color version of this figure is available only in the electronic edition.
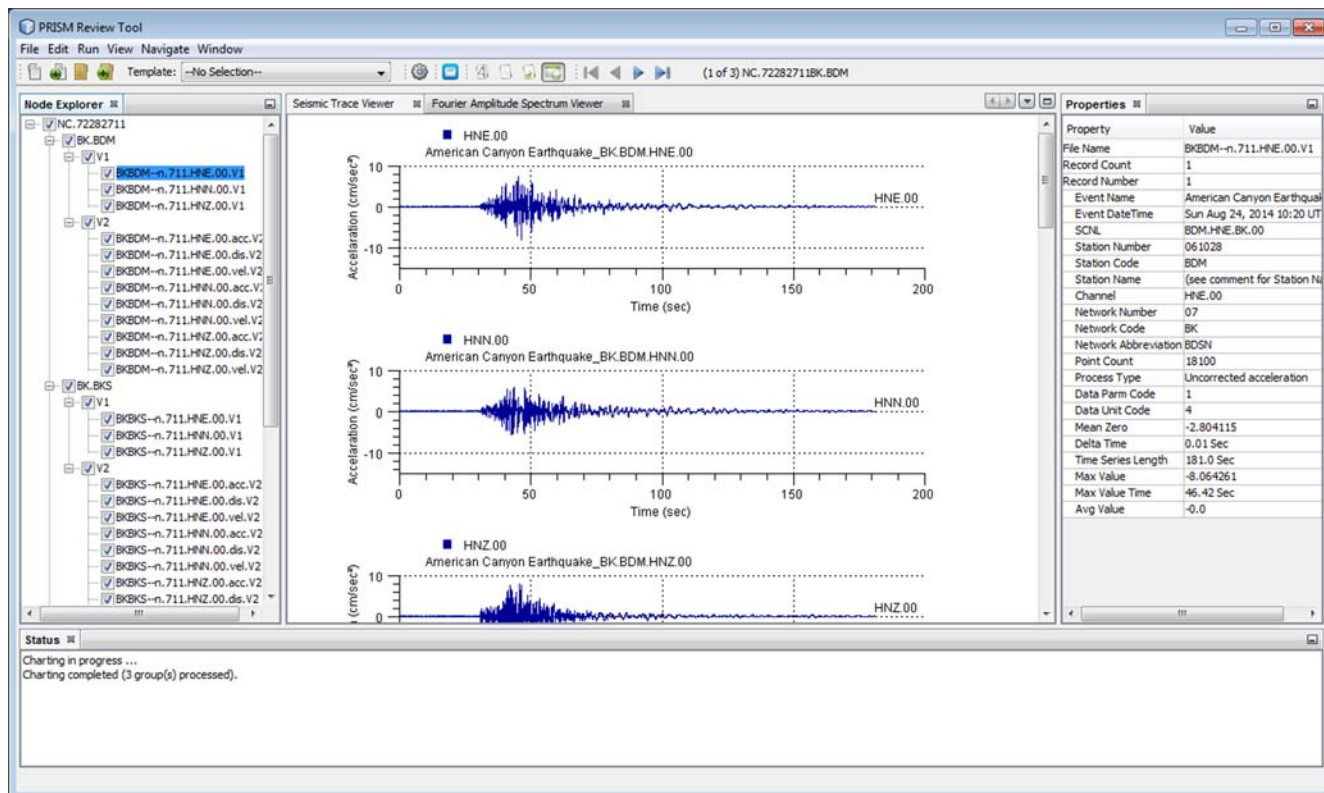
▲ **Figure 12.** Main interface of the PRISM review tool, which provides standard menu and toolbar options for performing common tasks, including setting application preferences, loading input files, generating plots, navigating plot sets, and editing. The color version of this figure is available only in the electronic edition.
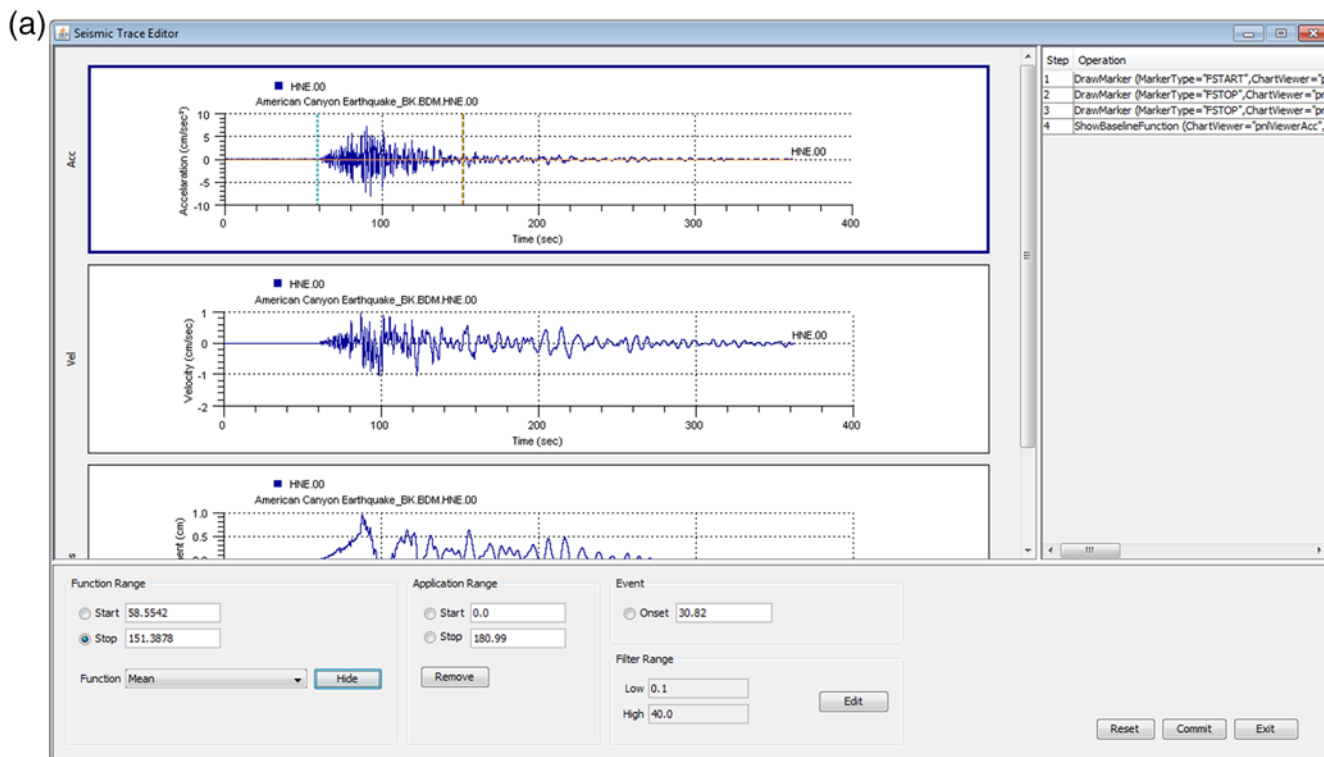
▲ **Figure 13.** (a) *Seismic Editor* and (b) *Fourier Amplitude Spectrum Editor* of the PRISM review tool to perform editing, baseline correction, and band-pass filtering of acceleration waveform. (*Continued*)
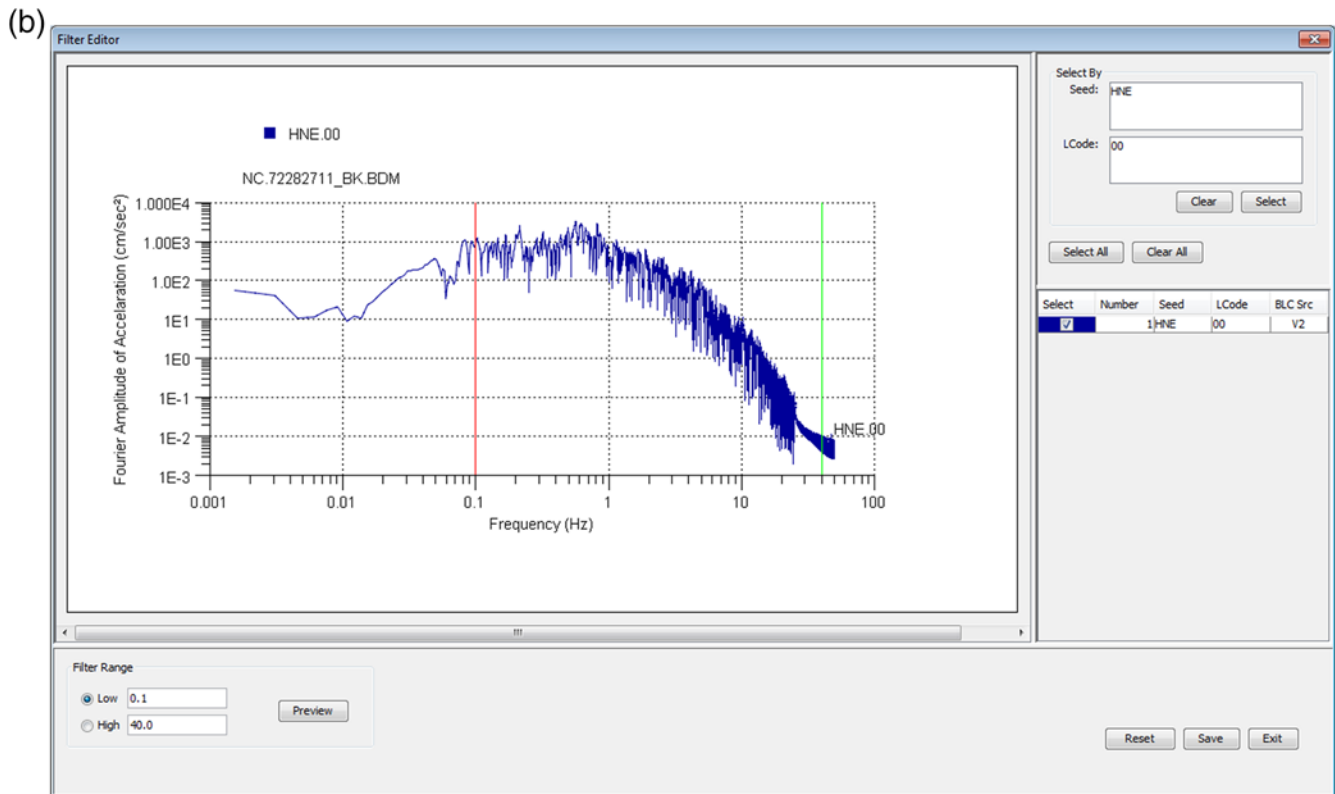
Figure 13. Continued.

ACKNOWLEDGMENTS

REFERENCES

Ancheta, T. D., R. B. Darragh, J. P. Stewart, E. Seyhan, W. J. Silva, B. S. J. Chiou, K. E. Wooddell, R. W. Graves, A. R. Kottke, D. M. Boore, *et al.* (2013). *PEER NGA-West Database, PEER Report 2013/03,* Pacific Earthquake Engineering Research Center, University of California, Berkeley, California.

Bazzurro, P., B. Sjoberg, N. Luco, W. Silva, and R. Darragh (2005). Effects of strong motion processing procedures on time histories, elastic and inelastic spectra, COSMOC publication: CP-2005/02, available online at http://www.cosmos-eq.org/publications/reports/CP-2005-02.pdf (last accessed March 2017).

Boore, D. M. (2001). Effect of baseline correction on displacements and response spectra for several recordings of the 1999 Chi-Chi, Taiwan, earthquake, *Bull. Seismol. Soc. Am.* **91,** no. 5, 1199–1211.

Boore, D. M. (2005). On pads and filters: Processing strong-motion data, *Bull. Seismol. Soc. Am.* **95,** no. 2, 745–750.

Boore, D. M., and S. Akkar (2003). Effect of causal and acausal filters on elastic and inelastic response spectra, *Earthq. Eng. Struct. Dynam.* **32,** 1729–1748.

Boore, D. M., and J. J. Bommer (2005). Processing of strong-motion accelerograms: Needs, options and consequences, *Soil Dynam. Earthq. Eng.* **25,** 93–115.

Boore, D. M., A. A. Sisi, and S. Akkar (2012). Using pad-stripped acausally filtered strong-motion data, *Bull. Seismol. Soc. Am.* **102,** no. 2, 751–760.

Boore, D. M., C. D. Stephens, and W. B. Joyner (2002). Comments on baseline correction of digital strong motion data: Examples from the 1999 Hector Mine California earthquake, *Bull. Seismol. Soc. Am.* **92,** no. 4, 1543–1560.

Boroschek, R. L., and D. Legrand (2006). Tilt motion effects on the double-time integration of linear accelerometers: An experimental approach, *Bull. Seismol. Soc. Am.* **96,** no. 6, 2072–2089.

Brune, J. N. (1970). Tectonic stress and the spectra of seismic shear waves from earthquakes, *J. Geophys. Res.* **75,** 4997–5009.

Brune, J. N. (1971). Correction, *J. Geophys. Res.* **76,** no. 20, 5002.

Consortium of Organizations for Strong-Motion Observation Systems (2001). *COSMOS Strong Motion Data Format*, 16 pp., available

at http://www.strongmotioncenter.org/vdc/cosmos_format_1_20.pdf (last accessed February 2017).

Consortium of Organizations for Strong-Motion Observation Systems (2005). *Guidelines and Recommendations for Strong-Motion Record Processing and Commentary, COSMOS Publication CP-2005/01,* 30 pp., available at http://www.cosmos-eq.org/publications/reports/CP-2005-01.pdf (last accessed February 2017).

Converse, A. M., and A. G. Brady (1992). BAP: Basic strong-motion accelerogram processing software, version 1.0, *U.S. Geol. Surv. Open-File Rept. 92-296-A,* 174 pp., available at https://pubs.er.usgs.gov/publication/ofr92296A (last accessed February 2017).

Darragh, R. B., W. J. Silva, and N. Gregor (2004). Strong motion record processing procedures for the PEER Center, *Proc. of COSMOS Workshop on Strong-Motion Record Processing,* Richmond, California, 1–12.

Graizer, V. M. (1979). Determination of the true ground displacement by using strong motion records, *Izvestiya Phys. Solid Earth* **15,** 875–885.

Graizer, V. M. (2010). Strong motion recordings and residual displacements: What are we actually recording in strong motion seismology? *Seismol. Res. Lett.* **81,** 635–639.

Graizer, V. M. (2015). Effect of low-pass filtering and re-sampling on spectral and peak ground acceleration in strong motion records, *Proc. of the 15th World Conference on Earthquake Engineering,* International Association for Earthquake Engineering, Lisbon, Portugal, 24–28 September 2015.

Graizer, V. M. (2005). Effect of tilt on ground motion data processing, *Soil Dynam. Earthq. Eng.* **25,** no. 3, 197–204.

Iwan, W. D., M. A. Moser, and C. Y. Peng (1985). Some observations on strong-motion earthquake measurements using a digital accelerograph, *Bull. Seismol. Soc. Am.* **75,** 1225–1246.

Jones, J., E. Kalkan, and C. Stephens (2017). Processing and Review Interface for Strong Motion Data (PRISM)—Methodology and automated processing, Version 1.0.0, *U.S. Geol. Surv. Open-File Rept. 2017-1008,* 80 pp., doi: 10.3133/ofr20171008.

Kalkan, E. (2016). An automatic P-phase arrival-time picker, *Bull. Seismol. Soc. Am.* **106,** no. 3, 971–986, doi: 10.1785/0120150111.

Kalkan, E., and V. Graizer (2007a). Coupled tilt and translational ground motion response spectra, *J. Struct. Eng.* **133,** no. 5, 609–619.

Kalkan, E., and V. Graizer (2007b). Multi-component ground motion response spectra for coupled horizontal, vertical, angular accelerations and tilt, *ISET J. Earthq. Technol.* **44,** no. 1, 259–284.

Kalkan, E., and S. K. Kunnath (2006). Effects of fling-step and forward directivity on the seismic response of buildings, *Earthq. Spectra* **22,** no. 2, 367–390.

Kalkan, E., and C. Stephens (2017). Systematic comparisons between PRISM, BAP and CSMIP ground-motion processing, *U.S. Geol. Surv. Open-File Rept. 2017–1020,* 108 pp., doi: 10.3133/ofr20171020.

Kanasewich, E. R. (1981). *Time Sequence Analysis in Geophysics,* Third Ed., Univ. Alberta Pr., Edmonton, Alberta.

Maeda, N. (1985). A method for reading and checking phase times in auto-processing system of seismic wave data, *Zisin* **38,** no. 3, 365–379.

Massa, M., F. Pacor, L. Luzi, D. Bindi, G. Milana, F. Sabetta, A. Gorini, and S. Marcucci (2010). The ITalian ACcelerometric Archive (ITACA): Processing of strong-motion data, *Bull. Earthq. Eng.* **8,** no. 5, 1175–1187.

Nigam, N. C., and P. C. Jennings (1969). Calculation of response spectra from strong-motion earthquake records, *Bull. Seismol. Soc. Am.* **59,** no. 2, 909–922.

SeismoSoft (2016). *SeismoSignal,* available at www.seismosoft.com (last accessed February 2017).

Shakal, A., M. J. Huang, and V. Graizer (2004). California Strong-Motion Instrumentation Program Processing Methods and Procedures, *Proc. of COSMOS Invited Workshop on Strong-Motion Processing,* 111–122, in COSMOS Pub. CP-2004/02, 246 pp.

Shakal, A. F., and J. T. Ragsdale (1984). Acceleration, velocity and displacement noise analysis for the CSMIP accelerogram digitization system, *Proc. of the 8th World Conference on Earthquake Engineering,* Vol. 2, 111–118.

Shakal, A. F., M. J. Huang, and V. M. Graizer (2003). Strong-motion data processing, in *International Handbook of Earthquake and Engineering Seismology, B,* W. H. K. Lee, H. Kanamori, P. C. Jennings, and C. Kisslinger (Editors), Academic Press, Amsterdam, The Netherlands, 967–981.

Stephens, C., and D. Boore (2004). USGS: ANSS/NSMP Strong-Motion Record Processing Methods and Procedures, *Proc. of COSMOS Invited Workshop on Strong-Motion Processing,* 123–130, in COSMOS Pub. CP-2004/02, 246 pp.

Trifunac, M. D. (1971). Zero baseline correction of strong-motion accelerograms, *Bull. Seismol. Soc. Am.* **61,** 1201–1211.

Trifunac, M. D. (1977). *Uniformly Processed Strong Earthquake Ground Accelerations in the Western United States of America for the Period from 1933 to 1971: Pseudo Relative Velocity Spectra and Processing Noise, Report No. 77-04,* Department of Civil Engineering, University of Southern California, Los Angeles, California, 219 pp.

Wang, L. J. (1996). *Processing of Near-Field Earthquake Accelerograms,* California Institute of Technology (unpublished), available at http://resolver.caltech.edu/CaltechEERL:1996.EERL-96-04 (last accessed February 2017).

Jeanne Jones
Peter Ng
Western Geographic Science Center
U.S. Geological Survey
345 Middlefield Road, MS 531
Menlo Park, California 94025 U.S.A.
jmjones@usgs.gov
png@usgs.gov

Erol Kalkan
Christopher Stephens
Earthquake Science Center
U.S. Geological Survey
345 Middlefield Road, MS 977
Menlo Park, California 94025 U.S.A.
ekalkan@usgs.gov
cdstephens@usgs.gov